Routledge
Taylor & Francis Group

Science & Global Security

The Technical Basis for Arms Control, Disarmament, and Nonproliferation Initiatives

ISSN: (Print) (Online) Journal homepage: https://www.tandfonline.com/loi/gsgs20

Flight Performance Analysis of the Samad Attack Drones Operated by Houthi Armed Forces

Mark Voskuijl , Thomas Dekkers & Ralph Savelsberg

To cite this article: Mark Voskuijl , Thomas Dekkers & Ralph Savelsberg (2020): Flight Performance Analysis of the Samad Attack Drones Operated by Houthi Armed Forces, Science & Global Security

To link to this article: https://doi.org/10.1080/08929882.2020.1846279

Published online: 10 Dec 2020.

SCIENCE & GLOBAL SECURITY
https://doi.org/10.1080/08929882.2020.1846279

Routledge
Taylor & Francis Group

Flight Performance Analysis of the Samad Attack Drones Operated by Houthi Armed Forces

Mark Voskuijl, Thomas Dekkers, and Ralph Savelsberg

Faculty of Military Sciences, Netherlands Defence Academy, Den Helder, The Netherlands

ABSTRACT

In recent years, there has been a large increase in the use of uncrewed attack aircraft, or attack drones, in the Yemen conflict. At the same time, the flight endurance and payload capabilities of these uncrewed aerial vehicles seem to have increased significantly. This article presents a flight performance analysis of the Samad aircraft family operated by Ansar Allah, the Houthi rebel movement. The analysis is based on information available in the public domain and accounts for modeling uncertainties, and terrain under weather conditions typical for Yemen and Saudi Arabia. With only limited data available in the form of images, the analysis method assesses the flight performance of fixed-wing attack aircraft with high aspect ratio wings and powered by piston engines and propellers. Results demonstrate that it is highly unlikely that the Samad-2 version could reach strategic locations in Saudi Arabia when launched from Houthi-controlled territory. The analysis shows that Samad-3, however, can achieve a flight range in excess of 1800 km, bringing Riyadh and oil installations near the Persian Gulf into reach. The results of the study can be used to predict the locations from which the Samad UAV can be deployed in an attack. Furthermore, it gives insight into the increasing threat of this type of UAV when employed by non-state actors. The methods and tools developed in this study can be used to analyze the capabilities of other UAV with similar configurations.

Introduction

On the morning of 14 September 2019, Saudi oil installations in Khurays and Abqaiq were attacked by at least 18 small uncrewed aerial vehicles (UAV) and 7 land-attack cruise missiles.[1] Khurays and Abqaiq are located approximately 1000 and 1200 km, respectively, from Houthi controlled territory. Saudi Arabia was surprised by this attack despite the presence of its sophisticated air defense systems. It has been suggested that the air defense systems were not prepared to detect small aircraft flying at low altitudes.[2] Although the attacks were claimed by Houthi rebels, Saudi Arabia, and the United States blamed Iran.[3]

CONTACT Mark Voskuijl m.voskuijl@mindef.nl Faculteit Militaire Wetenschappen, Nederlandse Defensie Academie, Het Nieuwe Diep 8, Den Helder 1781 AC, The Netherlands

Since 2018, Houthi forces have deployed at least three types of UAV: the Samad-2, the Samad-3, and an unnamed design with a delta wing. The Samad-3 is an upgraded version of the Samad-2 with an external fuel tank mounted on top of the fuselage. The Samad-2 and Samad-3 are also referred to as UAV-X.[4]

A U.N. Panel of Experts on Yemen analyzed the attacks based on a rough estimate of the achievable flight range.[5] They came to the conclusion that the flight range of UAV models available to the Houthis is too short to have been launched from within Houthi-controlled territory and reach these targets. Additionally, the installations were hit from the north-northwest and the north-northeast, whereas a strike from Houthi territory would originate from the south or southwest. Finally, the panel concluded that the Houthi forces were unlikely to be capable of launching such a precise and complex attack.

> "The Panel therefore concludes that, despite their claims to the contrary, the Houthi forces did not launch the attacks on Abqaiq and Khurays on 14 September 2019."[6]

In their yearly reports, the U.N. Panel of Experts on Yemen publishes basic information on the various UAV operated by Ansar Allah.[7] Several images of these UAV have been reported in the media.[8]

There were multiple reports of UAV attacks on various facilities. Not all reports, however, provide information about the types of UAVs used in an attack. The exact types of UAVs used in the attacks of 14 September 2019 are still unclear. The facilities in Abqaiq were hit by at least 18 uncrewed attack aircraft and the facilities in Khurays by at least four land-attack cruise missiles.[9] On 17 August 2019, oil fields in Shaybah were attacked by 10 UAVs.[10] The U.N. Panel of Experts inspected one of these vehicles and identified it as a Samad-3. The distance from Houthi-controlled territory to the oil fields in Shaybah is even greater than the distance to Abqaiq and Khurays. Long-range attacks were also staged on oil pumping facilities in Dawadimi and Afif on 14 May 2019.[11] The unnamed design with a delta wing is reported to be used in the attacks on 14 May 2019, as well as in the attack on Abqaiq on 14 September 2019. Regardless of who initiated the attacks on Saudi Arabia, they highlight the rapid improvements over the past years in the capabilities of UAV and cruise missiles. Houthi armed forces are known to have access to some of these UAVs.

Ansar Allah uses other types of UAV for surveillance, reconnaissance, and attacks. The Qasef-1 and the Qasef-2K are used as loitering munition, whereas the Hudhud-1 and the Rased are used as reconnaissance vehicles.[12] All were in use prior to 2018 and each has a shorter range than the Samad-2, Samad-3, and the unnamed delta wing design.

The aim of this analysis is to estimate the achievable flight range of the Samad aircraft family under weather conditions (e.g. wind, temperature,

and terrain) typical for Yemen and Saudi Arabia. Even though the unnamed design with a delta wing may also have a long flight range, it is not included in the analysis because there is a lack of information on this vehicle. Land-attack cruise missiles are also frequently used in attacks by Houthi forces but a performance analysis of cruise missiles is not included in the current research because it requires a different modeling approach.

The flight performance of the Samad aircraft family is analyzed using a combination of (1) methods traditionally employed within the early aircraft design phases, (2) statistical methods to account for uncertainties in aircraft design parameters, (3) detailed numerical flight simulations to replicate the attacks and other relevant scenarios, and (4) methods recently published on the design, sizing and analysis of UAVs. To strike a long-range target with a high level of precision requires accurate terminal guidance but that is not investigated here.

The remainder of this article presents a summary of the technical data available in the public domain, such as images of the aircraft that yield information about the UAVs dimensions and a flight simulation model based on the available data. The simulation models aerodynamic characteristics, propulsion systems, and the mass of the Samad family of aircraft under typical operating conditions for the region.

The results of the study can be used to predict the locations from which the Samad UAV can be deployed in an attack. Furthermore, it gives insight in the increasing threat of this type of UAV, which can be employed by non-state actors. Finally, the methods and tools developed in this study can be used in the future, to analyze the capabilities of other UAV with similar configurations.

Technical data

The Samad UAV family consists of the Samad-1, Samad-2, and Samad-3. The Samad-1 is used for surveillance and reconnaissance. Samad-2 appears to have the same aeronautical design but is larger and has an explosive payload of 18 kg. The Samad-3 is a modified version of Samad-2 with an external fuel tank that gives it an extended range. A few images of the Samad UAVs can be found in the public domain. The most detailed and reliable information is reported by the U.N. Panel of Experts on Yemen.[13] An image of the Samad-2 is provided in Figure 1.[14] It has a length of 2.80 m and a wing span of 4.50 m. The reported circumference of the fuselage is 84 cm. According to the U.N. report, the volume of the Samad-2 fuel tank is 21 L. Two types of engines are used to power the rear-mounted propeller: the German-made 3W110i B2 engine and the Chinese-made DLE

Figure 1. Reconstruction of Samad-2, length of 2.80 m (left); Samad-1 including details of the airfoil shape at the wing root (right).[15]

Figure 2. Motor and propeller (left); Samad-3 (front) and Samad-1 (back) on a display in Sana'a Yemen (right).[16]

170 engine. The Samad-3, with an external fuel tank mounted on top of fuselage, can be seen in Figure 2.

With the data reported by the United Nations and additional images found in the media, the shape and dimensions of the Samad-2 and Samad-3 aircraft can be estimated. The main wing has no sweep, dihedral or twist angle. The taper ratio equals 0.75 and the wing root chord is 34 cm. The image of a crashed Samad-1 (Figure 1) provides information on the type of airfoil used for the wing. Assuming that all Samad versions have the same aerodynamic design for the main wing, it is estimated that a profile similar to the NACA 23018 airfoil is used for the wing root and a profile similar to the NACA 23009 airfoil, with a smaller thickness over chord ratio, is used at the wing tip. The airfoils are presented in Figure 3.

Based on the image of the Samad-3 (Figure 2) and an image of a reconstructed Samad-3 documented in the latest report by the U.N. Panel of Experts on Yemen,[17] it is estimated that the external fuel tank has an ellipsoid shape with a volume of 26.3 ± 3.3 L. The ellipsoid has two semi-axes of 0.16 m and one semi-axis of 1.0 m. The propeller (Figure 2) has a fixed pitch and a diameter of 30 or 32 inches. This propeller design is in line with the recommendations of the engine manufacturers. As can be seen in

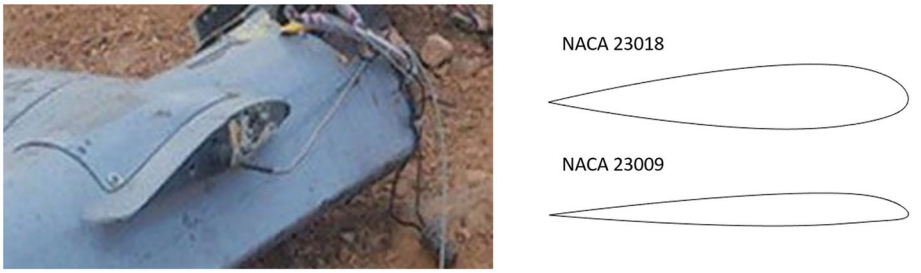

Figure 3. Close-up of Samad-1 (in Figure 1) showing the wing root airfoil (left); NACA 23018 airfoil and NACA 23009 (right).

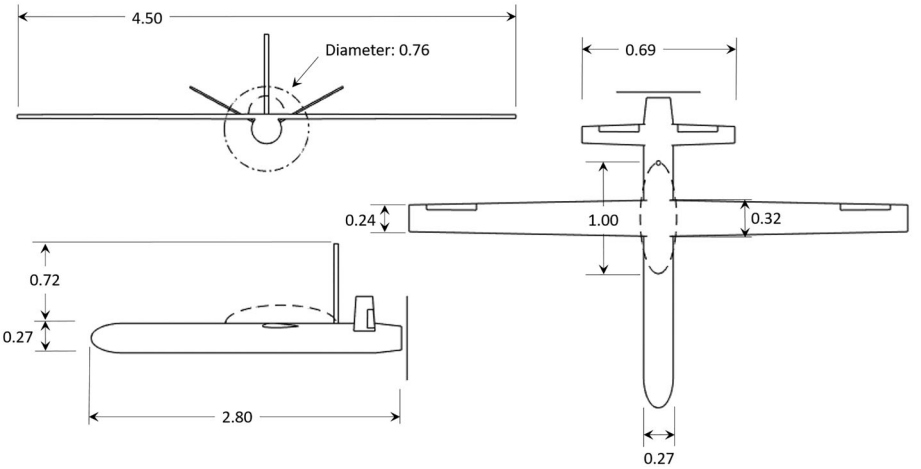

Figure 4. Schematic representation of the Samad-2 and Samad-3. The external fuel tank on the Samad-3 is indicated with a dashed line. The dash-dotted line in the front view on the top left shows the diameter of the propeller.

Figures 1 and 2, all three Samad variants have a prominent dorsal antenna, with a length of 72 cm and a diameter of 4 cm, which will result in a significant aerodynamic drag. Finally, the V-tail of the aircraft has a dihedral of 28 degrees (0.5 radians), no sweep angle or twist angle, and a taper ratio of 0.75. A schematic drawing of the Samad-2 and Samad-3 is presented in Figure 4. It can be observed in that the fuselage is assumed to have a circular cross section. Although the shape of the cross-section has no influence on the models used to analyze the aerodynamic performance and the weight of the vehicle in the following section it is important that the circumference of the fuselage is accurate. The circumference of the Samad-2 fuselage in Figure 1 is 84 cm.[18]

Flight performance simulation model

The simulation model used to analyze the Samad aircraft family consists of sub-models for the weight, aerodynamics, propulsion system, and

atmospheric conditions. Based on these sub-models, the equations of motion can be solved to compute the trajectory of the aircraft for a given flying strategy. The various sub-models are described in the following sections.

Aircraft geometry and mass

The mass of the aircraft plays an important role in the flight performance, or range estimates. In this study, methods traditionally used in aircraft design are used in reverse to determine the mass of the Samad aircraft family. The aircraft design process starts with the definition of "top-level aircraft requirements." These requirements define payload limits, range, and airspeed at cruise flight. It is standard practice in the conceptual and preliminary aircraft design phase to estimate the maximum take-off mass of the aircraft based on the top-level aircraft requirements and statistical data of aircraft with a similar role and configuration. In the more detailed design phases, the mass estimation of the primary structure is based on detailed physics-based structural analysis methods. Some modern approaches combine empirical methods and physics-based structural analysis methods.[19] The definition of the surface area and planform of the initial wing design and the available thrust are based on aircraft performance requirements during the design process. In case of the Samad-2 and Samad-3, the payload mass, wing surface area and planform and the available thrust are known. Hence, the design methods described above can be reverse engineered to estimate the maximum take-off mass. However, for this method to be successful, a statistical database of aircraft with a similar role and configuration must be available. Recently, a comprehensive article was published by Verstraete et al. that describes the relationship between maximum take-off mass, payload mass, wing area, wing span, and installed engine power for fixed-wing UAV with internal combustion engines.[20] Based on this dataset, an estimate is made of the operational empty mass of the Samad-2 and Samad-3 aircraft. The operational empty mass is defined as the mass of the complete aircraft excluding payload and fuel. Hence, it includes the mass of the engine, the aircraft structure, masses of secondary systems such as avionics, batteries, oil, unusable fuel, etc. The mass estimate consists of a mean value and a standard deviation. Since both designs feature the same wing planform and have the same payload, the estimate of the operational empty mass is identical. Samad-3 likely has a larger operational empty mass due to the structure of the fuel tank and additional elements such as piping. This difference is accounted for by the standard deviation in the mass estimate. The Samad-1, used solely for surveillance and reconnaissance purposes, appears to have a smaller size. Little

Table 1. Estimated mass breakdown of the Samad-2 and Samad-3 including modeling uncertainties.

	Mean mass $\bar{m}$ (kg)	Standard deviation σ (kg)
Operational empty mass Samad-2 and Samad-3 (including the mass of the motor of 4.3 kg)	53.6	12.5
Payload Samad-2 and Samad-3	18	0
Fuel Samad-2	15.9 (21 liter)	0.13
Fuel Samad-3	35.7 (47.3 liter)	0.96
Maximum take-off mass Samad-2	87.5	
Maximum take-off mass Samad-3	107.4	

information about the dimensions of the Samad-1 is publicly available. Binnie estimates a wingspan of 3.5 m for Samad-1.[21] If this is correct, it will have a shorter flight range as a consequence of aircraft scaling laws. The remainder of this article focuses on the weaponized versions of the Samad aircraft family. An overview of the mass breakdown is presented in Table 1.

Standard deviations are only provided for components and not for the maximum take-off mass, since a variation in the fuel mass not only affects the total mass but also directly the operating time of the engine.

Aerodynamics

The aerodynamic characteristics of an aircraft can be represented with a lift-drag polar, a parabolic equation that represents the relationship between aerodynamic drag and lift in a non-dimensional form. It describes the amount of aerodynamic drag for a given amount of lift. The aerodynamic lift must balance the aircraft weight in equilibrium conditions such as cruise flight. The lift-drag polar is written in a specific form to accurately model the aerodynamic characteristics of the Samad-2 and Samad-3 aircraft.

$$C_{\mathrm{D}} = C_{\mathrm{D}}^{*}(M) + K_{\mathrm{L}}(M)\left(C_{\mathrm{L}} - C_{\mathrm{L}}^{*}(M)\right)^{2} + C_{D_{\mathrm{antenna}}}(M) \tag{1}$$

where C_{D} is the drag coefficient and C_{L} is the lift coefficient. The drag coefficient consists of two parts. A lift dependent part (lift-induced drag) and a part independent of lift (parasitic drag). The Samad aircraft have a relatively large antenna for communications. The drag coefficient of the antenna ($C_{\mathrm{D,antenna}}$) is therefore represented separately from the other elements of the airframe (wing, fuselage and empennage). $C_{\mathrm{D}}{}^{*}$ is the minimum drag coefficient of the airframe without antenna which occurs at a specific lift coefficient designated $C_{\mathrm{L}}{}^{*}$. K_{L} is a parameter that describes the increase in the drag coefficient for a given increase in the lift coefficient. The parameters in the lift-drag polar are a function of the Mach number M. The non-dimensional drag coefficient C_D and lift coefficient C_L are

multiplied by the wing surface area (S), and dynamic pressure ($\frac{1}{2}\rho V^2$) to produce the drag and lift force expressed in Newtons.

$$D = C_D \frac{1}{2}\rho V^2 S \tag{2}$$

$$L = C_L \frac{1}{2}\rho V^2 S \tag{3}$$

where V is the airspeed and ρ is the air density. The lift-drag polar described above is a so-called three-term lift-drag polar—the aerodynamics of the airframe is characterized by three separate (Mach number dependent) parameters ($C_D{}^*$, $C_L{}^*$, and K_L). In various studies and textbooks on aircraft performance, a simpler form of the lift-drag polar is used with only two terms ($C_L{}^*$ equals zero) which are independent of the Mach number. The specific form of the lift-drag polar in the current study is needed to enable mission simulations with a sufficient level of accuracy.[22] How the different parameters in the lift-drag polar are determined for the Samad-2 and Samad-3 aircraft is described below.

The drag coefficient of the antenna ($C_{D,antenna}$) is estimated with ESDU method 83025.[23] This empirical method is based on an extensive set of experimental data of cylinders in a large range of flight conditions. Several methods are used to estimate the parameters representing the lift-induced drag coefficient (K_L and $C_L{}^*$) and the parasitic drag coefficient for the aircraft without antenna ($C_D{}^*$). One method that computes the lift-induced drag coefficient and the parasitic drag coefficient is called DATCOM. It is a well-known semi-empirical method, capable of producing fast results in the preliminary design phases.[24] Shafer analyzed the accuracy of DATCOM when applied to a fixed-wing UAV with a conventional configuration.[25] According to Shafer, lift prediction is accurate and drag prediction is reasonable, especially in the linear lift region. The variation of lift with angle of attack is almost linear in normal operating conditions such as cruise and high-speed flight. The combination of the DATCOM method with the ESDU method for the antenna drag is designated *aerodynamic model A* in this study. Another approach for computing the parasitic drag coefficient of the airframe is the "handbook" methods. The handbook methods of Torenbeek, Shevell, Raymer, and Hoerner use a component build-up technique.[26] For each primary component of the aircraft (fuselage, wing, and tail surfaces), the parasitic drag is estimated based on the drag of a flat plate with the same wetted area as the element and a similar boundary layer development. A form factor is defined to account for the shape of the component. Corrections are applied to account for interference between components. Factors used in the equations are defined for different aircraft categories and are based on extensive empirical data sets. These datasets, however, do not (yet) exist for small fixed-wing UAV. According to Götten

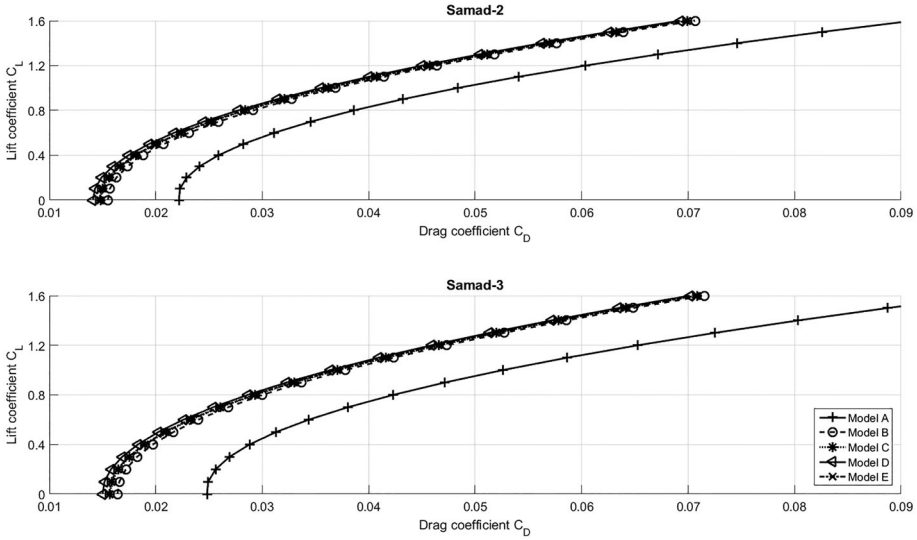

Figure 5. Lift-drag polars of the Samad-2 and Samad-3 at Mach 0.10 for different aerodynamic modeling approaches.

et al., drag coefficients of small to medium-sized reconnaissance UAVs are higher than the predictions made by the handbook methods.[27] Hence, the aerodynamic characteristics predicted by Torenbeek, Shevell, Raymer, and Hoerner are expected to be on the optimistic side. The handbook methods described above are frequently applied in the early design stages and must be combined with a separate method to predict the lift-induced drag to obtain a complete lift-drag polar. The "Athena Vortex Lattice" method (AVL) is selected to estimate the lift-induced drag.[28] AVL is accurate for aircraft with relatively thin lifting surfaces and a high aspect ratio, operating at low subsonic Mach numbers. This applies to the Samad aircraft configuration. The handbook methods of Torenbeek, Shevell, Raymer, and Hoerner in combination with AVL to predict lift-induced drag and ESDU to estimate antenna drag are designated as aerodynamic model B, C, D, and E, respectively.

The lift-drag polars of Samad-2 and Samad-3 at a Mach number of 0.10 (34 m/s at standard sea-level conditions) are provided in Figure 5 for the different aerodynamic models. This Mach number is close to the cruise speed which will be demonstrated in the results section.

Aerodynamic model A predicts maximum lift over drag ratios of 20.8 and 19.1 for the Samad-2 and Samad-3, respectively. The reduced aerodynamic performance of the Samad-3 can be attributed to the external fuel tank because it increases the frontal area and the wetted area of the fuselage. Models B–E, which are likely optimistic, predict a lower parasitic drag coefficient for the airframe. Since models B–E provide similar results, only results obtained with aerodynamics models A and B are presented here.

Propulsion system

The propulsion system of the Samad aircraft family consists of a piston engine combined with a fixed-pitch propeller. According to a report by the U.N. Panel of Experts, two types of engines are used on the Samad: the Chinese-made DLE 170 and the German-made 3W110i B2.[29] All Samad-2 aircraft analyzed by the panel was powered by the DLE 170. According to the engine manufacturer, it has a maximum power of 17.5 horsepower at 7500 rpm. The associated maximum fuel flow is 6.5 liter per hour. The standard deviation of the maximum fuel flow is assumed to be 0.17 liters per hour. This estimate is based on the maximum reported fuel flow variation by the manufacturer. The engine idle speed is 1100 rpm. The effect of flight altitude on the maximum shaft power (P_{br}) provided by the engine is modeled with the following relation.[30]

$$P_{\mathrm{br,max}} = P_{\mathrm{br,max_0}}\left(\frac{\rho}{\rho_0}\right) \tag{4}$$

In this equation, the subscript 0 indicates sea level conditions. The air density (ρ) decreases with altitude and thereby the shaft power as well. The available thrust provided by the isolated propeller (without the airframe) is determined by the ESDU method as a function of airspeed and altitude.[31] This established method is based on an extensive set of wind tunnel data of propellers. Correlations between measurement data of different propeller designs and predictions made by the method show that estimations for 90% of the cases considered are within 10% of the measured data. The propeller dimensions and rotational speed of the Samad aircraft family are within the recommended bounds of the ESDU method. Thrust computations of the isolated propeller with an accuracy within ±10% of the thrust is therefore expected. It is assumed that the pitch of the propeller is selected by the designers of the aircraft, such that the maximum rpm is achieved at the maximum level flight speed of the aircraft. The thrust calculated by the ESDU methods is uninstalled. In other words, it is the thrust of the propeller without the presence of the airframe, such as in a controlled wind tunnel experiment of an isolated propeller. In reality, blockage effects occur because the propeller is located at the rear of the fuselage. This leads to a reduction in thrust when installed on the aircraft.

$$T_{\mathrm{installed}} = \eta T_{\mathrm{uninstalled}} \tag{5}$$

The installation loss factor (η) is assumed to be 0.8 with a standard deviation of 0.017, based on the experimental research published by Verstraete and MacNeill.[32] The available installed thrust as a function of airspeed and flight altitude is presented in Figure 6. The atmospheric conditions (pressure, density, and temperature as a function of altitude) are based on the

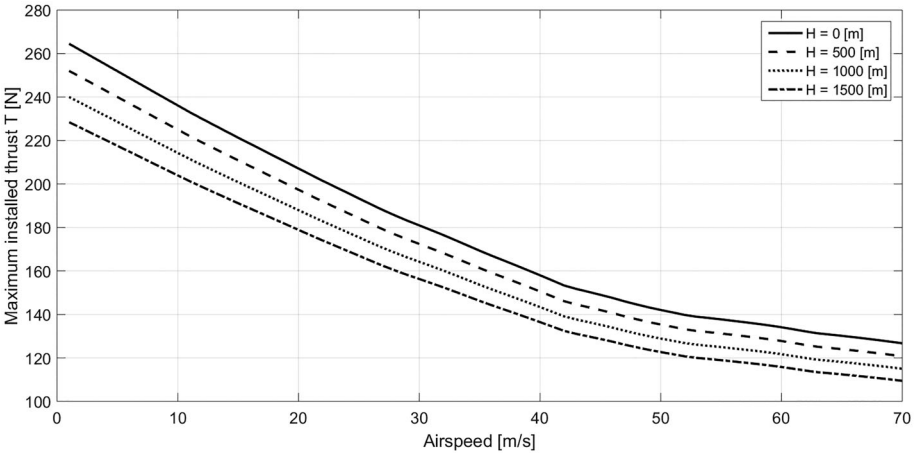

Figure 6. Available installed thrust delivered by the propulsion system.

International Standard Atmosphere (ISA) on a standard day. This atmospheric model is based on the ideal gas law, a hydrostatic equilibrium, and an empirical relation for the temperature variation with altitude.

The static uninstalled thrust at 100 m altitude, calculated with the ESDU method, is within 5% of the value (35 kg) that can be expected according to the engine manufacturer.[33]

Mission simulation

The trajectory of the aircraft is simulated with the point mass equations of motion. The flight path is discretized over 60 s intervals. Throughout the flight, which typically has a duration of more than 5 h, there are variations in speed and flight path angle. These variations are small enough to assume that the accelerations at individual time intervals are zero. Hence, the flight is assumed to be quasi-steady and symmetric. This results in the following equations of motion.

$$L = W\cos\gamma + T\sin(\alpha + i) \tag{6}$$

$$T\cos(\alpha + i) = D + W\sin\gamma \tag{7}$$

These equations are defined parallel and perpendicular to the airspeed vector (V) which has a flight path angle (γ) with respect to the horizon. The aerodynamic force is represented by two components; lift (L) and drag D. The aircraft weight is represented with the variable W. The thrust vector (T) has an angle (i) with respect to the aircraft body axis. Finally, the aircraft has an angle of attack (α) relative to the airflow. The kinematic equations include terms to account for wind components parallel (V_{headwind}) and perpendicular ($V_{\text{crosswind}}$) to the prescribed flight path with respect to

the ground. The set of kinematic equations relative to the ground is presented below.

$$V_{x,\text{ground}} = V\cos\gamma\cos\chi - V_{\text{headwind}} \tag{8}$$

$$V_{y,\text{ground}} = V\cos\gamma\sin\chi - V_{\text{crosswind}} \tag{9}$$

$$V_{z,\text{ground}} = V\sin\gamma \tag{10}$$

The azimuth angle of the airspeed vector (χ) is defined relative to the prescribed path of the mission. The x-component of the ground speed is parallel to the prescribed path from one waypoint of the mission to the next. Hence, the y-component of the ground speed must be zero for or it will drift from the prescribed path. The vertical component of the speed (rate of climb/descent – $V_{z,\text{ground}}$) must be controlled such that the correct altitude is maintained. This vertical component of the speed is typically small or close to zero since a typical mission profile has a gradual climb and descent phase. In some cases however, a terrain following mission may require significant climb or descent rates.

Results of the flight performance analysis

The simulation model presented in the previous section analyzes several scenarios. In the following section the range of the Samad-2 and Samad-3 is calculated in ideal conditions (no wind). Next, the effect of atmospheric conditions, such as headwind, tailwind, and temperature, is analyzed. Finally, the attack of the Khurays oil installations is simulated, considering the weather conditions on the day of the attack and the altitude profile of the terrain between Houthi-controlled territory and the oil installations.

Range in standard conditions

The range of the Samad-2 and Samad-3 is first computed for standard atmospheric conditions (ISA) without wind at a night and early morning average air temperature of 25 °C typically encountered in Saudi Arabia. Low-level flights at a constant pressure altitude (500 m) are evaluated. The airspeed profile is optimized along the trajectory to achieve maximum range. As the aircraft weight slowly decreases due to fuel burn, the airspeed is slowly reduced to maintain the optimal conditions to achieve maximum range. The fuel consumption during take-off and the initial climb phase is neglected. The effects of the aerodynamic model and uncertainty in the mass prediction on the estimated flight range are included in the analysis using Monte Carlo simulations. Also included are uncertainties in two propulsion system parameters, the propeller installation loss and the fuel flow of the engine when operating at its maximum power setting. Results for

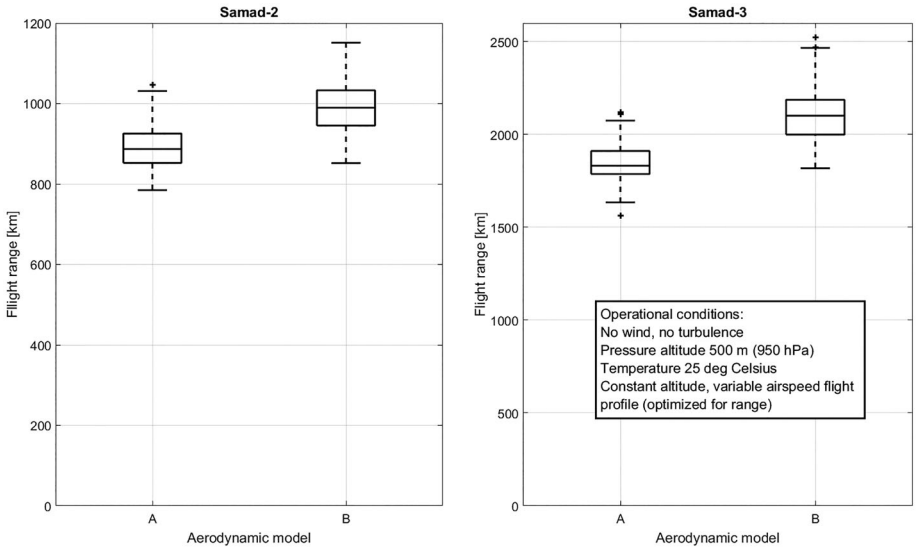

Figure 7. Effect of uncertainty of simulation model parameters (take-off mass of the aircraft, fuel tank volume, propeller installation loss, and power specific fuel consumption of the engine) on the estimated flight range of the Samad-2 and Samad-3 for different aerodynamic modeling approaches.

the Samad-2 and Samad-3 are presented in Figure 7. The central horizontal line in each box represents the median. The top and bottom edges of a box indicate the 75th and 25th percentiles, respectively. The whiskers extend to the maximum and minimum values. The crosses are outliers in the data.

The median of the estimated flight range of the Samad-2 varies between 887 km for aerodynamic model A and 989 km for aerodynamic model B. For both models, the data between the minimum value for the 25th percentiles and the maximum value for the 75th percentiles have a range of 852–1033 km. Results for aerodynamic models C, D, and E are similar to aerodynamic model B and are therefore not displayed. This was expected since they rely on similar methods. The analyses reveal the same trends for the Samad-3. However, this aircraft has a significantly longer range due to the larger fuel tank. The fuel tank also has negative effects on the flight performance by increasing the frontal area and surface area of the fuselage, resulting in a somewhat increase in aerodynamic drag. In addition, the take-off mass is also increased. The median values of Samad-3 range from 1831 to 2101 km, extending the range by approximately 1000 km.

Based on the range calculations for the Samad-2, a crude estimate of the flight range of Samad-1 can also be made assuming it has a wing span of 3.5 m. Based on the smaller wing span, the statistical relations of Verstraete et al. predict that the maximum take-off mass of the Samad-1 is only 55% of the maximum take-off mass of Samad-2.[34] Verstraete et al. also provide a statistical relation for the product of payload and endurance as a function

Table 2. Effect of wind speed, temperature, and aerodynamic model on estimated range of Samad-2 for constant altitude flights at 500 m (pressure altitude).

Weather conditions	Wind direction	Tailwind		No wind		Headwind	
	Wind speed (m/s)	−10	−5	0	0	5	10
	Temperature (°C)	25	25	25	10	25	25
Aerodynamic model	A	1144	1014	891	898	774	666
	B	1270	1121	978	987	838	711

Airspeed is optimized along the trajectory to achieve maximum range. The mass and propulsion system parameters are set at their mean values.

of maximum take-off mass. This relation predicts that the product of payload and endurance of the Samad-1 equals 38% of the product of payload and endurance of Samad-2. Since the Samad-1 has a smaller payload, smaller size, and slower flight speed, it is estimated to have a flight range of approximately 460 km. This estimation is based on aircraft scaling laws and an assumed payload of 10 kg. This result corresponds with a claim made in a Houthi video which states the flight range of the Samad-1 is 500 km.[35]

Effect of weather conditions

The Samad aircraft operate at relatively low airspeeds compared to manned aircraft due to their size. Consequently, wind conditions can have a significant influence on flight performance. The effect of wind speed on the achievable range is presented in Table 2 for the Samad-2. Also included is a single analysis of the effect of temperature by simulating a relatively cold day with no wind. In this sensitivity analysis, the take-off mass and propulsion system parameters are all set at their baseline (mean) values.

From Table 2, wind conditions have a significant effect on the achievable flight range. Under favorable wind conditions, range can be extended by approximately 200 km. Temperature effects on flight performance are minor. The flight range on a cold day, early in the morning can be approximately 20–30 km more than in warmer conditions. It should be noted that to obtain these results at non-zero wind conditions, the flight speed of the aircraft is continuously optimized to achieve maximum range (with respect to the ground). If flights are conducted at a constant airspeed, the range will be approximately 1–2% less than what is reported in Table 2.[36] If flights are conducted at higher airspeeds to reach the target faster, flight range will also be reduced.

Simulation of attacks on Khurays oil installations (14 september 2019)

The attacks on the Khurays oil installations on the early morning of 14 September 2019 are simulated with models of the Samad-2 and Samad-3 aircraft. Two sites were attacked (Khurays and Abqaiq) and it was reported

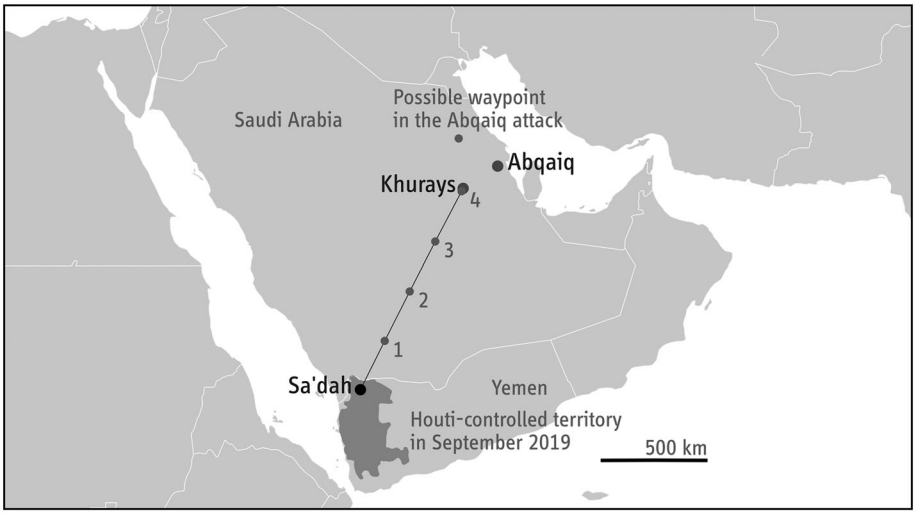

Figure 8. Simulated mission from Houthi-controlled territory near the border of Saudi Arabia to the Khurays oil installations on 14 September 2019. Waypoints for the simulated attack are displayed and details are provided in Table 3.

Table 3. Flight profile and atmospheric conditions for mission from Houthi-controlled territory to Khurays oil installations on the evening of 13 September to the morning of 14 September.

Waypoint	Range (km)	Altitude above mean sea level (m)	Headwind (m/s)	Crosswind (m/s)	Temperature (°C)
Sa'dah	0	2126	3.98	3.46	29.0
1	250	1237	4.61	4.01	35.5
2	500	925	5.53	1.86	35.5
3	750	886	0.48	6.93	32.0
4	1000	703	−2.37	2.73	30.0
Khurays	1014	444	−2.19	2.52	30.5

that Khurays was hit by at least 4 land-attack cruise missiles and Abqaiq by at least 18 weaponized UAV. Abqaiq is further away that Khurays is largely the same direction. If these simulations indicate that Samad aircraft cannot reach Khurays then they cannot reach Abqaiq. Khurays was therefore selected for a detailed simulation even though there is no confirmation of a strike by an UAV there.

The simulated mission path (represented in Figure 8 and Table 3) followed various waypoints to the target under actual weather conditions for the day of the flight.[37] The primary sources of the meteorological data reported by Ventusky are the National Oceanic and Atmospheric Administration (NOAA) and the German Weather Service (DWD). Other country-specific meteorological data sources are also consulted. The launch site of the mission is unknown and is assumed to be in the region of the city of Sa'dah, approximately 50 km from the northwestern border of

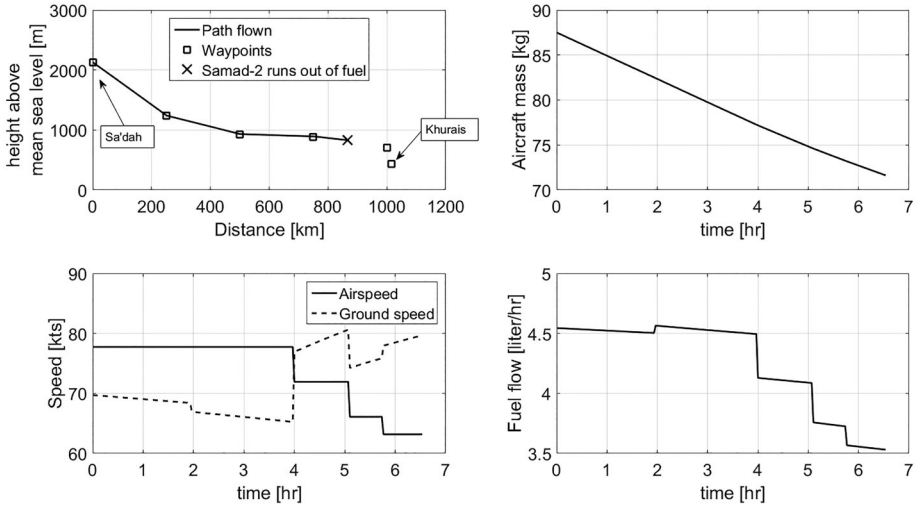

Figure 9. Simulated mission to Khurays oil field with Samad-2 (take-off mass: 87.5 kg, aerodynamic model A, propeller installation loss factor: 80%, fuel flow at maximum shaft power: 6.5 L/h).

territory controlled by Houthi in September 2019. A map of the territory controlled by the Houthi forces is shown in Figure 8. The defined mission results in a gradually descending flight with headwinds at the start and tailwinds in the final stages. The location of the other site which was attacked (Abqaiq) is indicated in Figure 8. The report by the U.N. Panel of Experts mentions that one of the UAVs used in the Abqaiq attack had a waypoint programmed that was northwest of Abqaiq. The location of this waypoint is indicated in Figure 8 as well. It should be noted that this information could not be verified by the United Nations.

During the first part of the mission, the aircraft encounters headwinds and crosswinds. A low-level flight, 250 m above ground, is conducted in which the altitude of the terrain is followed until the Khurays oil installations are reached and the aircraft descends to ground level. Airspeed throughout the flight was optimized to achieve the greatest range possible. In summary, it is a gradually descending flight with a small headwind and crosswind on a warm day with a total flight range of 1014 km. Key flight performance parameters for simulations with Samad-2 and Samad-3 are presented in Figures 9 and 10.

It can be observed in Figure 9 that the Samad-2 runs out of fuel approximately 150 km from the Khurays oil installations after a total flight time of 6 h and 34 min, even using airspeed optimization. It is more likely that a suboptimal path would be flown at a constant airspeed resulting in an even smaller flight range. The Samad-2 is capable of successfully completing this simulation mission with an unlikely (although not impossible) combination of parameters: most optimistic aerodynamic model, lowest propeller

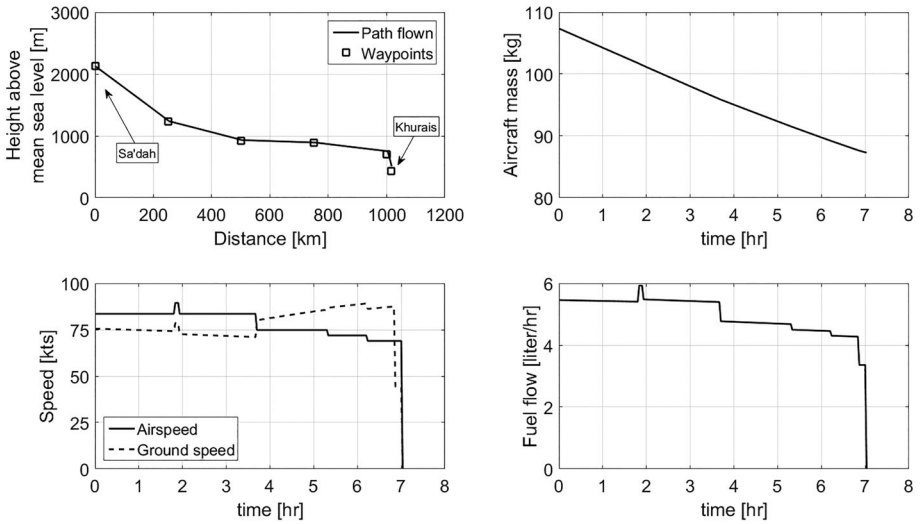

Figure 10. Simulated mission to Khurays oil field with Samad-3 (take-off mass: 107.4 kg, aerodynamic model A, propeller installation loss factor: 80%, fuel flow at maximum shaft power: 6.5 L/h).

installation loss, most fuel-efficient engine estimate, and lowest aircraft weight. Given their inability to reach Khurays, the simulation demonstrates that a Samad-2 UAV attack on Abqaiq oil fields launched from Houthi controlled territory was not possible. The Samad-3 on the other hand is capable of reaching Khurays. With the same simulation model settings, it reaches Khurays after 7 h with 44% of the fuel remaining. The simulation models predict that Abqaiq is also within the flight range of the Samad-3 considering the weather conditions on 14 September 2019 and a terrain following flight.

The 2019 report of the U.N. Panel of Experts on Yemen mentions another (unsuccessful) attack executed with the Samad (UAV-X).

> "The Panel received information that one UAV-X had crashed within 30 km of Riyadh after having run out of fuel, although Saudi Arabia publicly denied that the attack took place."[38]

Riyadh is about 100 km closer to Houthi-controlled territory than the Khurays oil installations in a straight flight. Which type of Samad that crashed is unclear. It may have been a Samad-2 that ran out of fuel, but it could also have been a Samad-3 that malfunctioned. If it was indeed a Samad-2, the event seems to confirm the model results in Figure 9. It should be noted that the weather conditions are not known during this attempted attack on Riyadh.

Discussion and summary of results

The results of this research indicate that the attacks on the Khurays and Abqaiq oil installations on 14 September 2019 could not have been

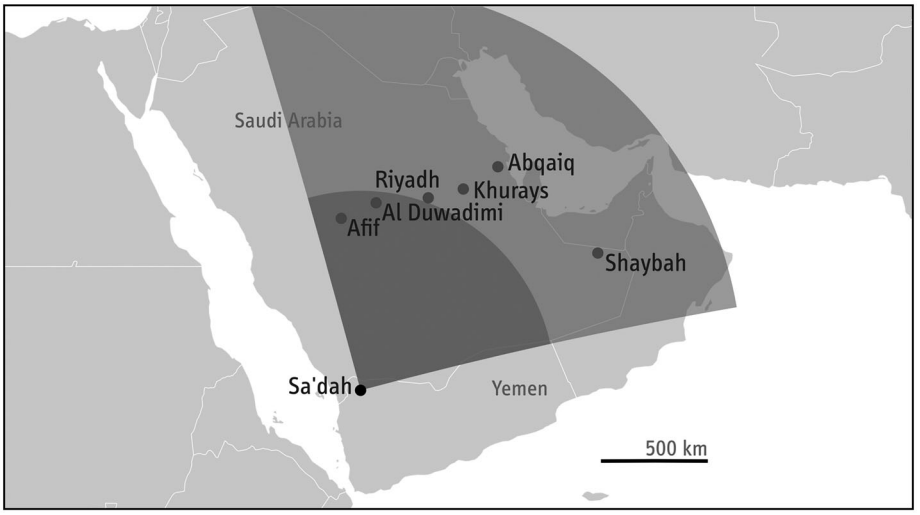

Figure 11. Flight range of the Samad-2 and Samad-3 when launched from Sa'dah in the direction of targets which were attacked in 2019. The simulated ranges displayed are estimated based on aerodynamic model A and all baseline model values without the presence of wind.

conducted with Samad-2 UAVs launched from within Houthi-controlled territory. Using reasonable performance and operational conditions, the Samad-2 does not have the required range and simply cannot fly that far. However, the simulation models do demonstrate that the Samad-3 UAV has sufficient flight range to attack the Khurays and Abqaiq oil installations from the same launch site. The extended range of the Samad-3 brings strategic targets such as oil installations near the Persian Gulf and Riyadh within reach. The flight range of the Samad-2 and Samad-3 UAVs is shown in Figure 11. The ranges shown are at optimum conditions and the flight range can be increased or decreased by 200 km depending on the wind conditions. For the analysis of specific attacks, weather conditions on the day of the attack should therefore be considered.

Even though the analysis demonstrates the flight performance capabilities of the Samad aircraft family, to stage a successful high precision attack an accurate terminal guidance system is required.

Conclusions and recommendations

The simulation models developed for this analysis can be used to replicate specific events and incorporate actual weather conditions. Detailed flight performance models of the Samad-2 and Samad-3 aircraft are developed based on technical data (primarily images) available in the public domain. The effect of uncertainties of various modeling parameters on the predicted flight performance is addressed using Monte Carlo simulations. The modeled results show that it is highly unlikely that the Samad-2 aircraft

launched from Houthi controlled territory attacked the Khurays, Abqaiq, and Shaybah oil installations in 2019. However, the Samad-3 with its external fuel tank and extended range could have reached these strategic targets.

This new analysis method can be utilized to analyze other UAV designs with similar roles and configurations. The models could also be used to monitor further development in the conflict in Yemen. Finally, since this analysis did not consider guidance systems, but that such systems might limit the achievable flight range, further investigation of mid course and terminal guidance is recommended.

Notes and References

1. The attacks were reported in various news media. The following three articles provide a good overview: Seth J. Frantzman, "Are air defense systems ready to confront drone swarms?" *DefenseNews*, 26 September 2019, https://www.defensenews.com/global/mideast-africa/2019/09/26/are-air-defense-systems-ready-to-confront-drone-swarms/. Shawn Snow, "Drone and missile attacks against Saudi Arabia underscore need for more robust air defenses," *Military Times*, 25 October 2019, https://www.militarytimes.com/flashpoints/2019/10/25/drone-and-missile-attacks-against-saudi-arabia-underscore-need-for-more-robust-air-defenses/; Nikolay Kozhanov, "The attacks on Aramco could hurt Saudi Arabia in the long term," *Al Jazeera*, 4 October 2019, https://www.aljazeera.com/indepth/opinion/attacks-aramco-hurt-saudi-arabia-long-term-191002120641621.html; "Final report of the Panel of Experts on Yemen," United Nations Security Council, S/2020/326, 28 April 2020, 82–84.
2. Seth J. Frantzman, "Are air defense systems ready to confront drone swarms?"
3. It is debated in various news media who was behind the attacks on Khurays and Abqaiq. The following two articles give more details. Patrick Wintour and Julian Borger, "Saudi offers 'proof' of Iran's role in oil attack and urges US response," *The Guardian*, 18 September 2019, https://www.theguardian.com/world/2019/sep/18/saudi-oil-attack-rouhani-dismisses-us-claims-of-iran-role-as-slander. Lisa Barrington and Aziz El Yaakoubi, "Yemen Houthi drones, missiles defy years of Saudi air strikes," *Reuters World News*, 17 September 2019, https://www.reuters.com/article/us-saudi-aramco-houthis/yemen-houthi-drones-missiles-defy-years-of-saudi-air-strikes-idUSKBN1W22F4.
4. "Final report of the Panel of Experts on Yemen," S/2020/326, 28 April 2020, 21–23.
5. "Final report of the Panel of Experts on Yemen," S/2020/326, 28 April 2020, 87–89.
6. "Final report of the Panel of Experts on Yemen," S/2020/326, 28 April 2020, 87–89.
7. The United Nations Panel of Expert on Yemen produces a yearly report with detailed information on air strikes conducted with uncrewed attack aircraft and the design of these aircraft. Paragraph IV.C and annexes 37 and 38 of the 2018 report give a detailed overview of the short-range uncrewed attack aircraft in use. "Final report of the Panel of Experts on Yemen," United Nations Security Council, S/2018/68, 26 January 2018. The longer-range designs are first mentioned in paragraph IV.B and Annex 12 of the 2019 report, "Final report of the Panel of Experts on Yemen," United Nations Security Council, S/2019/83, 25 January 2019. The most detailed design information on the Samad-3 and the new Delta design UAV is presented in

paragraph III.A of the 2020 report, "Final report of the Panel of Experts on Yemen," S/2020/326, 28 April 2020.

8. Various images of an exhibition in which Houthi attack drones and land attack cruise missiles are displayed are presented in the following article, UAE's Yemen Troop Withdrawal Follows New Houthi Weapons, Threats of Attack on Dubai," Ahmed AbdulKareem, *Islam Times* (11 July 2019), https://www.islamtimes.org/en/article/804353/uae-s-yemen-troop-withdrawal-follows-new-houthi-weapons-threats-of-attack-on-dubai. Video showing the capabilities of Houthi Drones can be seen at the UAV DACH – Unmanned Aviation Association website, https://www.uavdach.org/?p=1295670.
9. "Final report of the Panel of Experts on Yemen," S/2020/326, 28 April 2020, 82–84.
10. "Final report of the Panel of Experts on Yemen," S/2020/326, 28 April 2020, 21.
11. "Final report of the Panel of Experts on Yemen," S/2020/326, 28 April 2020, 20–22.
12. The Qasef and Rased short range uncrewed attack aircraft are described in paragraph IV.C of the "Final report of the Panel of Experts on Yemen," S/2018/68, 26 January 2018. All short-range vehicles are presented in more detail in paragraph IV.B of: Final report of the Panel of Experts on Yemen," S/2019/83, 25 January 2019.
13. The weaponized version of the Samad UAV is first reported under the name UAV-X in paragraph IV.B of the "Final report of the Panel of Experts on Yemen," S/2019/83, 25 January 2019. More detailed information of the Samad-2 and Samad-3 is reported in paragraph III.A of the "Final report of the Panel of Experts on Yemen," S/2020/326, 28 April 2020.
14. "Final report of the Panel of Experts on Yemen," S/2019/83, 25 January 2019, 88–91.
15. "The joint resistance forces in Hodeidah shot down an UAV of the Houthis west of the city of Tahita," Live Universal Awareness Map, 4 April 2019, https://yemen.liveuamap.com/en/2019/4-april-the-joint-resistance-forces-in-hodeidah-shot-down.
16. "The joint resistance forces in Hodeidah shot down an UAV of the Houthis west of the city of Tahita," Live Universal Awareness Map, 4 April 2019, https://yemen.liveuamap.com/en/2019/4-april-the-joint-resistance-forces-in-hodeidah-shot-down. The image was reported by different news media such as Al Arabiya and the Saudi Press Agency, https://english.alarabiya.net/en/News/gulf/2019/08/13/Arab-Coalition-Houthis-fired-a-drone-from-Sana-a-that-landed-in-Amran.html *Al Arabiya*, 14 August 2019, https://english.alarabiya.net/en/News/gulf/2019/08/13/Arab-Coalition-Houthis-fired-a-drone-from-Sana-a-that-landed-in-Amran.html. "Political / Joint Forces Command of the Coalition "Coalition to Support Legitimacy in Yemen." The terrorist Houthi militia launched a drone (booby trapped) from Sana'a governorate and landed in Amran governorate on civilian objects," *Saudi Press Agency*, 13 August 2019, https://www.spa.gov.sa/1958280.
17. "UAE's Yemen Troop Withdrawal Follows New Houthi Weapons and Threats of Attack on Dubai," *Yemen-Press News Agency*, 23 July 2019; "Final report of the Panel of Experts on Yemen," S/2020/326, 28 April 2020, 22.
18. "Final report of the Panel of Experts on Yemen," S/2019/83, 25 January 2019, 88.
19. Ali Elham, Gianfranco La Rocca and Michel J. L. van Tooren, "Development and implementation of an advanced, design-sensitive method for wing weight estimation," *Aerospace Science and Technology* 29(1) (2013): 100-113, https://doi.org/10.1016/j.ast.2013.01.012.
20. Dries Verstraete, Jennifer L. Palmer and Mirko Hornung, "Preliminary Sizing Correlations for Fixed-Wing Unmanned Aerial Vehicle Characteristics," *Journal of Aircraft* 55 (2018): 715–726, https://doi.org/10.2514/1.C034199.

21. Jeremy Binnie (@jeremybinnie), "My crude dimensional analysis based on the first photo indicates the Sammad-3 has roughly the same wingspan (4.5m) as the 'UAV-X' recovered in Saudi Arabia & UAE, the Sammad-1 thus being closer to 3.5m," Twitter, 8 July 2019, https://twitter.com/JeremyBinnie/status/1148255599731384320.
22. Egbert Torenbeek, *Advanced Aircraft Design: Conceptual Design, Analysis and Optimization of Subsonic Civil Airplanes* (New Jersey: John Wiley & Sons Ltd., 2013), 95–98.
23. "Drag of circular cylinders normal to a flat plate with turbulent boundary layer for Mach numbers up to 3," Engineering Sciences Data Unit, ESDU Data Item 83025, August 1983.
24. John E. Williams and Steven R. Vukelich, "The USAF Stability and Control Digital DATCOM, Volume I, User's Manual," AFFDL-TR-79-3032, November 1979.
25. Theresa C. Shafer et al., "Comparison of computational approaches for rapid aerodynamic assessment of small UAVs," 52nd AIAA Aerospace Sciences Meeting - AIAA Science and Technology Forum and Exposition, SciTech, National Harbor, Maryland, 2014, https://doi.org/10.2514/6.2014-0039.
26. Since the 1960s various handbook methods for conceptual and preliminary aircraft design were developed. The methods of Torenbeek, Shevell, Raymer, and Hoerner are widely used. Egbert Torenbeek, *Synthesis of Subsonic Airplane Design* (Rotterdam: Nijgh-Wolters-Noordhoff Universitaire Uitgevers B.V., 1976), 487–519. Richard S. Shevell, *Fundamentals of Flight* (Pearson, 1989); Daniel P. Raymer, *Aircraft Design: A Conceptual Approach* (Washington, D.C.: American Institute for Aeronautics and Astronautics Education Series, 1992) 280–297; Sighard F. Hoerner, *Fluid-Dynamic Drag. Theoretical, experimental and statistical information* (Hoerner Fluid Dynamics, 1965).
27. Falk Götten et al., "On the applicability of empirical drag estimation methods for unmanned air vehicle design," *18th AIAA Aviation Technology Integration and Operations Conference*, Atlanta, 2018, https://doi.org/10.2514/6.2018-3192.
28. Marc Drela and Harold Youngren, "Athena Vortex Lattice," Accessed on 22 May 2020, http://web.mit.edu/drela/Public/web/avl/.
29. "Final report of the Panel of Experts on Yemen," S/2019/83, 25 January 2019, 30–31.
30. Ger J. J. Ruijgrok, *Elements of Airplane Performance* (VSSD, 2009), 196.
31. The ESDU method used to determine the thrust of a fixed pitch propeller under various operating conditions consists of two data items. "Approximate Parametric Method for Propeller Thrust Estimation," Engineering Sciences Data Unit, ESDU Data Item 83001, November 1983; "Approximate Parametric Method for Propeller Thrust Estimation – Addendum A: Application to Fixed-Pitch Propellers," Engineering Sciences Data Unit, ESDU Data Item 83028, November 1983.
32. D. Verstraete and R. MacNeill, "The Effects of Blockage on the Performance of Small Propellers," 20thAustralasian Fluid Mechanics Conference, Perth, Australia, 5–8 December 2016.
33. "DLE 170," https://www.dlengine.com/en/rcengine/dle170.
34. Dries Verstraete, Jennifer L. Palmer and Mirko Hornung, "Preliminary Sizing Correlations for Fixed-Wing Unmanned Aerial Vehicle Characteristics." 2018.
35. Jeremy Binnie (@jeremybinnie), "My crude dimensional analysis based on the first photo indicates the Sammad-3 has roughly the same wingspan (4.5m) as the 'UAV-X' recovered in Saudi Arabia & UAE, the Sammad-1 thus being closer to 3.5m," Twitter, 8 July 2019, https://twitter.com/JeremyBinnie/status/1148255599731384320.

36. Shiva K. Ohja, *Flight Performance of Aircraft* (Washington, D.C.: American Institute of Aeronautics and Astronautics, Inc., 1995), 237–256, https://doi.org/10.2514/4.861826.
37. Weather conditions were retrieved from a web based application called Ventusky which is developed by the company InMeteo. The primary sources of the meteorological data reported by Ventusky are the National Oceanic and Atmospheric Administration (NOAA) and the German Weather Service (DWD). Other country-specific meteorological data sources are also consulted. "Ventusky," https://www.ventusky.com.
38. "Final report of the Panel of Experts on Yemen," S/2019/83, 25 January 2019, 30.